

## 1 Rare decays of B-hadrons

---

**Carla Marin Benito**<sup>\*†</sup>

*Laboratoire de l'Accélérateur Linéaire*

*E-mail:* [carla.marin@cern.ch](mailto:carla.marin@cern.ch)

Rare decays of  $b$ -hadrons provide high sensitivity to New Physics effects. Several deviations with respect to the Standard Model predictions have been observed in recent years, leading to significant tensions in global fit analyses. It is thus crucial to update the existing measurements and study new decay modes to confirm the pattern. The latest results from LHCb and Belle on radiative, semileptonic penguin, lepton universality and lepton flavour violation decays are presented.

*XXIX International Symposium on Lepton Photon Interactions at High Energies - LeptonPhoton2019  
August 5-10, 2019  
Toronto, Canada*

---

<sup>\*</sup>Speaker.

<sup>†</sup>On behalf of the LHCb collaboration

## 1. Introduction

Rare decays of b-hadrons are Flavor-Changing Neutral-Currents (FCNC), which are forbidden at tree level in the Standard Model (SM) and are thus very suppressed. As such, they are very sensitive to potential new particles entering the loops virtually and affecting properties of the decays such as branching fractions and angular distributions. Consequently, the measurement of these processes allows to probe higher scales than direct searches. As an example, the Feynman diagram of the FCNC  $b \rightarrow s\gamma$  transition in the SM is shown in Fig. 1.

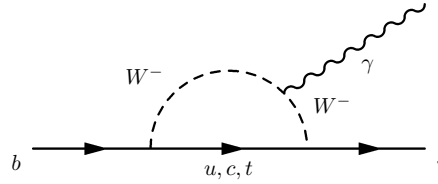


**Figure 1:** Feynman diagram of the FCNC  $b \rightarrow s\gamma$  transition in the SM.

From the theoretical viewpoint, these decays can be described in a model-independent way by means of the Operator Product Expansion. The effective Hamiltonian of the theory is expressed as a sum over all the possible operators, which are modulated by a set of coefficients, known as Wilson coefficients ( $C_i$ ). The most relevant effective couplings are those parametrising the vector ( $C_9$ ), vector-axial ( $C_{10}$ ) and photon mediated ( $C_7$ ) operators. The Wilson coefficients can be computed in the SM and compared to the values extracted from global fits to experimental data. Any significant deviation from the SM calculations taking into account both experimental and theory uncertainties would point to New Physics (NP) effects.

In recent years several deviations with respect to SM predictions have been observed in this type of processes. Differential branching fraction ( $\mathcal{B}$ ) measurements in  $b \rightarrow s\ell\ell$  decays exhibit a trend towards values lower than the SM predictions in the di-lepton mass squared,  $q^2$ , region below the charmonium threshold [1, 2, 3], although theoretical predictions for these observables are affected by large hadronic uncertainties. Deviations have been also observed in the theoretically cleaner  $P'_5$  angular observable in the  $B^0 \rightarrow K^{*0}\mu^+\mu^-$  decay [4]. Lepton Flavor Universality tests, which are complementary to these measurements and provide theoretically very precise observables, also show a deviation with respect to the universal SM prediction [5, 6].

In view of all these anomalies in rare b-hadron decays, it is crucial to update the previous measurements with more data and study new complementary modes. The most recent results from LHCb and Belle on rare b-hadron decays are reported in the following.

## 2. Radiative decays

Radiative decays of b-hadrons are mediated by the  $b \rightarrow s\gamma$  quark-level transition, governed by the  $C_7^{(\prime)}$  Wilson coefficient. The  $C_7$  coefficient is very constrained already by the measurement of the branching fraction of the inclusive  $B \rightarrow X_s\gamma$  process and of direct CP asymmetry in the  $B^0 \rightarrow K^{*0}\gamma$  decay. However, the presence of right-handed currents beyond the standard model in

33 this transition, entering in the  $C_7'$  coefficient, has only been mildly constrained so far. Experimentally, this can be tested through a measurement of the polarisation of the emitted photon, which is  
 34 predicted to be left-handed in the SM, up to corrections of the order  $m_s/m_b$ . Current studies focus  
 35 on the measurement of observables sensitive to the photon polarisation to improve the constraints  
 36 on potential new physics entering  $C_7'$ .  
 37

## 38 2.1 Photon polarisation in $B_s^0 \rightarrow \phi\gamma$

39 The time-dependent rate of a  $B_s^0$  meson decay to a CP even final state is given by the expres-  
 40 sion:

$$\Gamma(t) \propto \exp^{-\Gamma_s t} \left[ \cosh\left(\frac{\Delta\Gamma_s t}{2}\right) - A^\Delta \sinh\left(\frac{\Delta\Gamma_s t}{2}\right) \pm C_{CP} \cos(\Delta m_s t) \mp S_{CP} \sin(\Delta m_s t) \right] \quad (2.1)$$

41 where  $\Delta\Gamma_s$  and  $\Delta m_s$  are the width and mass differences between the two mass eigenstates and  $\Gamma_s$  is  
 42 their average width. The last two terms change the sign of their contribution depending on whether  
 43 the produced particle is a  $B_s^0$  meson or an anti- $B_s^0$  meson and thus one needs to know the flavour  
 44 of the hadron at production to measure them. The coefficients  $A^\Delta$  and  $S_{CP}$  are sensitive to the  
 45 photon helicity and weak phases, while  $C_{CP}$  is related to CP violation in the decay. Exploiting  
 46 the decay  $B_s^0 \rightarrow \phi\gamma$ , LHCb measured  $A^\Delta = -0.98^{+0.46+0.23}_{-0.52-0.20}$  using a dataset corresponding to  $3 \text{ fb}^{-1}$   
 47 collected in Run 1 of the LHC, in an analysis where no information on the flavour of the initial  
 48  $B_s^0$  was used [7]. Earlier this year, an updated measurement including flavour tagging information  
 49 was published [8]. The time-dependent decay rate of events tagged as  $B_s^0$ ,  $\overline{B}_s^0$  or with no tagging  
 50 information is fit separately to extract the coefficients entering Eq. 2.1, as shown in Fig. 2. The  
 51 obtained results are:

$$\begin{aligned} A^\Delta &= -0.67^{+0.37}_{-0.41} \pm 0.17 \\ C_{CP} &= 0.11 \pm 0.29 \pm 0.11 \\ S_{CP} &= 0.43 \pm 0.30 \pm 0.11, \end{aligned} \quad (2.2)$$

52 where the first uncertainty is statistical and the second systematic. The results are compatible with  
 53 the absence of right-handed currents and CP violation. This is the first measurement of the  $C_{CP}$  and  
 54  $S_{CP}$  coefficients in the  $B_s^0$  system.

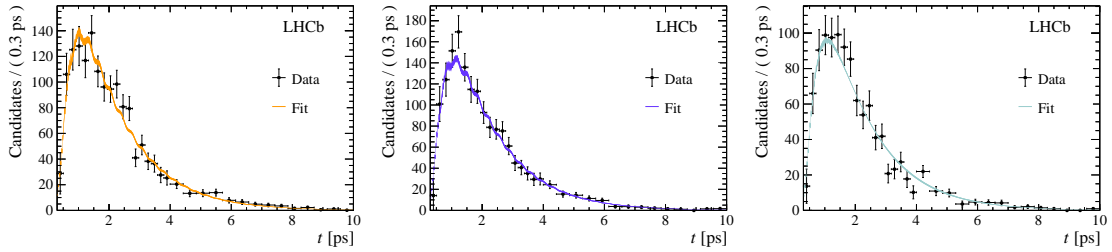


**Figure 2:** Time-dependent decay rate of  $B_s^0 \rightarrow \phi\gamma$  candidates for events tagged as  $B_s^0$  (left),  $\overline{B}_s^0$  (middle) and with no tagging information (right). The black points show the data and the results of the fit are represented by the solid curves.

## 55 2.2 First observation of $\Lambda_b^0 \rightarrow \Lambda \gamma$

56 The  $\Lambda_b^0 \rightarrow \Lambda \gamma$  decay is also a FCNC  $b \rightarrow s \gamma$  transition, which was previously unobserved. The  
 57 SM prediction for its branching ratio stands in the range  $10^{-7} - 10^{-5}$ , with the large uncertainty  
 58 originating from the computation of form factors [9, 10, 11, 12]. The best limit on this observ-  
 59 able was set by CDF at  $\mathcal{B}(\Lambda_b^0 \rightarrow \Lambda \gamma) < 1.9 \times 10^{-3}$  at 90% CL [13], which leaves large room  
 60 for experimental improvement to reach the SM prediction. This decay offers direct access to the  
 61 photon polarisation in  $b \rightarrow s \gamma$  decays through the angular distribution of the final state particles  
 62 and can thus probe the existence of right-handed currents [14]. LHCb has performed a search for  
 63 this decay mode using the dataset collected in 2016, which corresponds to  $1.7 \text{ fb}^{-1}$  of integrated  
 64 luminosity [15].

65 The particular topology of this decay poses a great challenge for its reconstruction at LHCb.  
 66 The  $\Lambda_b^0$  decay vertex, typically exploited to suppress prompt background, cannot be reconstructed  
 67 in this case due to the long lifetime of the  $\Lambda$  baryon and the lack of information on the direction  
 68 of the photon detected in the electromagnetic calorimeter. Consequently, a dedicated online and  
 69 offline reconstruction was developed to be able to study this mode, where the  $\Lambda_b^0$  momentum is  
 70 computed from the direct sum of the  $\Lambda$  and  $\gamma$  momenta, without a vertex fit. A large combina-  
 71 torial background is expected due to the impossibility of applying tight requirements on the  $\Lambda_b^0$   
 72 decay vertex and is mitigated with a high performance BDT trained using the XGBoost [16] algo-  
 73 rithm. Neutral particle identification tools [17] are exploited to reject potential background from  $\pi^0$   
 74 misidentification. Other sources of background, apart from a small contamination from  $\Lambda_b^0 \rightarrow \Lambda \eta$   
 75 decays with  $\eta \rightarrow \gamma \gamma$ , are found to be negligible.

76 The well-known  $B^0 \rightarrow K^{*0} \gamma$  decay is used as normalisation mode to extract a branching ratio  
 77 measurement using the recent measurement of the  $\Lambda_b^0$  hadronisation fraction ratio at 13 TeV by  
 78 LHCb [18]. The normalisation mode and intermediate state branching fractions are taken from the  
 79 PDG [19] and the efficiencies,  $\varepsilon$ , are computed from simulation and calibration samples.

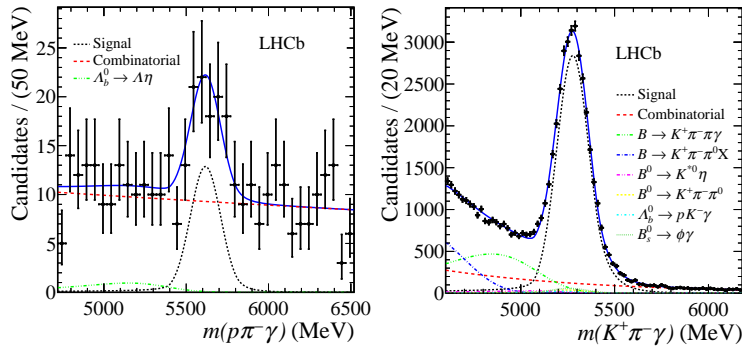


**Figure 3:** Invariant mass distribution of selected  $\Lambda_b^0 \rightarrow \Lambda \gamma$  (left) and  $B^0 \rightarrow K^{*0} \gamma$  (right) candidates (black dots). The result of a simultaneous unbinned maximum likelihood fit is shown by the blue curve, with different contributions represented by different style and color curves, as described in the legend.

80 The results of a simultaneous unbinned maximum likelihood fit to signal and normalisation  
 81 candidates are shown in Fig. 3. A clear signal peak of  $65 \pm 13$  events is observed, together with  
 82  $32670 \pm 290 B^0 \rightarrow K^{*0} \gamma$  events. The significance of the signal excess is found to be  $5.6\sigma$ , which  
 83 represents the first observation of the  $\Lambda_b^0 \rightarrow \Lambda \gamma$  decay mode. The branching fraction is measured

84 to be

$$\mathcal{B}(\Lambda_b^0 \rightarrow \Lambda \gamma) = (7.1 \pm 1.5 \pm 0.6 \pm 0.7) \times 10^{-6}, \quad (2.3)$$

85 where the first uncertainty is statistical, the second systematic and the third arises from external  
 86 inputs, which are dominated by the systematic uncertainties on the determination of the ratio of  
 87 hadronisation fractions. The measurement is well within the range of SM predictions and can be  
 88 used to determine the  $\Lambda_b^0 \rightarrow \Lambda$  form factors at the photon pole. With a larger dataset this decay  
 89 mode can be exploited to obtain a measurement of the photon polarisation in radiative b-baryon  
 90 decays.

### 91 3. Semileptonic penguin decays

92 Semileptonic  $b \rightarrow s \ell^+ \ell^-$  transitions are mediated by the  $C_7$ ,  $C_9$  and  $C_{10}$  Wilson coefficients in  
 93 the SM, in different proportions depending on the  $q^2$  region. The di-lepton spectrum is dominated  
 94 by the narrow charm resonances  $J/\psi$  and  $\psi(2S)$  that are typically excluded in analyses and used as  
 95 control modes instead. The main focus in this sector is on angular analyses and lepton flavour uni-  
 96 versality tests, both on the update of previous analyses with more data and improved experimental  
 97 techniques and on the measurement of these observables in new decay modes not explored before.

#### 98 3.1 Angular analysis of $\Lambda_b^0 \rightarrow \Lambda \mu^+ \mu^-$

99 The  $\Lambda_b^0 \rightarrow \Lambda \mu^+ \mu^-$  decay is a  $b \rightarrow s \ell^+ \ell^-$  transition complementary to  $B^0 \rightarrow K^{*0} \mu^+ \mu^-$  with  
 100 a richer angular distribution due to the half-integer spin of the baryons and the potential initial  
 101 polarisation of the  $\Lambda_b^0$  hadron. The analysis [20] is performed using the data recorded by LHCb in  
 102 the period 2011 – 2016, corresponding to an integrated luminosity of  $5 \text{ fb}^{-1}$ , and focuses on the low  
 103 recoil region,  $15 < q^2 < 20 \text{ GeV}^2/c^4$ , where most of the signal lies. The angular analysis exploits  
 104 the method of moments [21] to measure for the first time the full set of angular observables for this  
 105 decay. The 5-dimensional angular distributions are described by the sum of 35 angular functions,

$$\frac{d^5\Gamma}{d\Omega} = \frac{3}{32\pi^2} \sum_i^{34} K_i f_i(\Omega), \quad (3.1)$$

106 where  $K_i$  are the angular coefficients extracted from the fit to data. The results for these parameters  
 107 are shown in Fig. 4. All the coefficients are compatible with the SM predictions computed with  
 108 the EOS [22] software using the  $\Lambda_b^0$  production polarisation measured by LHCb [23]. The  $K_{11, \dots, 34}$   
 109 coefficients are found to be compatible with zero, i.e., with the absence of initial  $\Lambda_b^0$  polarisation.  
 110 Forward-backward asymmetries in the lepton and hadron systems and between the two systems  
 111 can be derived from the combination of different coefficients. They are found to be

$$A_{FB}^\ell = \frac{3}{2} K_3 = -0.39 \pm 0.04 \pm 0.01$$

$$A_{FB}^h = K_4 + \frac{1}{2} K_5 = -0.30 \pm 0.05 \pm 0.02$$

$$A_{FB}^{h\ell} = \frac{3}{4} K_6 = +0.25 \pm 0.04 \pm 0.01,$$

112 which are also in agreement with the SM predictions.

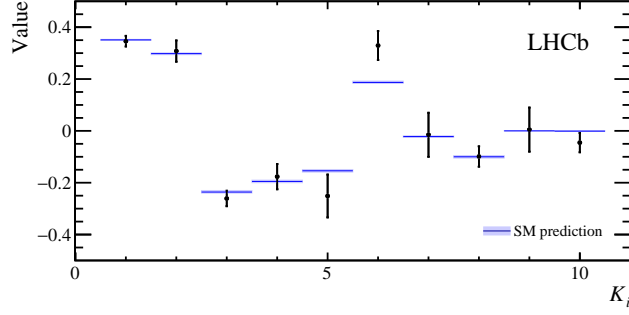


**Figure 4:** Angular coefficients of the  $\Lambda_b^0 \rightarrow \Lambda \mu^+ \mu^-$  decay obtained from the fit to data (black dots) and SM prediction (blue bands).

### 113 3.2 Lepton Universality Tests

114 Lepton universality tests in  $b \rightarrow s \ell^+ \ell^-$  transitions involve the comparison of muon and elec-  
 115 tron final states that share the same hadronic content, which in the SM are predicted to behave  
 116 exactly equal, except for the lepton masses. Experimentally, electrons and muons are detected very  
 117 differently, specially in a high momentum and occupancy environment such as the LHC, causing  
 118 reconstruction and selection differences than need to be carefully controlled.

119 At LHCb, the main differences arise from the way these events are triggered and from the  
 120 Bremsstrahlung losses that electrons suffer as they traverse the detector material. At the hardware  
 121 trigger level, electrons are selected as high energetic clusters in the electromagnetic calorimeter  
 122 (ECAL), while muons are distinguished by the traces they leave in the muon stations. Due to the  
 123 different occupancies of both detectors, a larger transverse momentum threshold is needed in the  
 124 ECAL to control the rate of selected events. This is mitigated by exploiting other parts of the event  
 125 to trigger on. In particular, the hadron from the  $b \rightarrow s \ell^+ \ell^-$  decay of interest or any high energetic  
 126 signature from the other  $b$  produced in the event are used.

127 A procedure is in place to correct the electron track momentum from potential Bremsstrahlung  
 128 losses. The direction of the track before the magnet is propagated to the ECAL surface and the  
 129 momenta of photon clusters near the extrapolated track position are added to the one measured  
 130 by the tracking. This provides a good recovery of a large fraction of the emitted energy but some  
 131 signal photons can be missed while others originating from different processes can be incorrectly  
 132 added, causing a degradation of the mass resolution for electron modes in comparison to muon  
 133 ones.

134 The ratio of branching fractions of a given  $b \rightarrow s \ell^+ \ell^-$  process with electrons or muons in the  
 135 final state is predicted in the SM to be

$$R_H = \frac{\mathcal{B}(H_b \rightarrow H_s \mu^+ \mu^-)}{\mathcal{B}(H_b \rightarrow H_s e^+ e^-)} = 1 \quad (3.2)$$

136 with a 1% accuracy [24]. Experimentally, one measures the yields of these two decays, which can  
 137 be related to the ratio of branching fractions through the reconstruction and selection efficiencies:

$$R_H = \frac{N(H_b \rightarrow H_s \mu^+ \mu^-)}{N(H_b \rightarrow H_s e^+ e^-)} \times \frac{\varepsilon(H_b \rightarrow H_s e^+ e^-)}{\varepsilon(H_b \rightarrow H_s \mu^+ \mu^-)}. \quad (3.3)$$

138 Event yields are obtained from invariant mass fits to data candidates, while efficiencies are com-  
 139 puted from simulation and calibration samples. In order to validate the correct description of the  
 140 data provided by the simulation, the corresponding  $J/\psi$  modes, which have been tested accurately  
 141 in the past to be flavour universal [19], are exploited. The ratio

$$r_{J/\psi} = \frac{\mathcal{B}(H_b \rightarrow H_s J/\psi (\mu^+ \mu^-))}{\mathcal{B}(H_b \rightarrow H_s J/\psi (e^+ e^-))} \quad (3.4)$$

142 provides a stringent cross-check. Moreover, at LHCb, the  $R_H$  ratios are measured as a double ratio  
 143 between the rare and  $J/\psi$  resonant modes, to ensure any potential systematics in the computation  
 144 of efficiencies cancel out.

145 An update of the measurement of the ratio  $R_K = \mathcal{B}(B^+ \rightarrow K^+ \mu^+ \mu^-) / \mathcal{B}(B^+ \rightarrow K^+ e^+ e^-)$  has  
 146 been published by LHCb early this year [25]. The analysis uses the dataset collected during  
 147 2011-2016, corresponding to an integrated luminosity of  $5 \text{ fb}^{-1}$ , and measures  $R_K$  in the region  
 148  $1.1 < q^2 < 6.0 \text{ GeV}^2/c^4$ . A re-optimisation of the analysis of the 2011-2012 dataset [5] is per-  
 149 formed together with the inclusion of new data not previously studied. In total, a factor 2 larger  
 150 statistics than in the previous analysis is obtained. The  $r_{J/\psi}$  cross-check is found to be in good  
 151 agreement with unity,  $r_{J/\psi} = 1.014 \pm 0.035$ . Moreover, this ratio is also measured in one and  
 152 two-dimensional bins of decay kinematics and no significant trends are observed, validating the  
 153 efficiency extraction from simulation and calibration samples. The invariant mass fits to  $K^+ \mu^+ \mu^-$   
 154 and  $K^+ e^+ e^-$  candidates are shown in Fig. 5. The broader signal shape for the electron mode re-  
 155 quires the usage of a larger fit range and the inclusion of more backgrounds in the fit model. In  
 156 particular, partially reconstructed events of the type  $B^0 \rightarrow K^{*0} e^+ e^-$  with  $K^{*0} \rightarrow K^+ \pi^-$ , where the  
 157  $\pi^-$  is not reconstructed, and contamination from the  $J/\psi$  mode due to large Bremsstrahlung losses  
 158 are significant in this case. In total, around 1940 and 760  $B^+ \rightarrow K^+ \mu^+ \mu^-$  and  $B^+ \rightarrow K^+ e^+ e^-$   
 159 events are observed. Taking into account the reconstruction and selection efficiencies, the ratio of  
 160 branching fractions between the two modes is measured to be

$$R_K = 0.846_{-0.054-0.014}^{+0.060+0.016}, \quad (3.5)$$

161 where the first uncertainty is statistical and the second systematic. This value is compatible with  
 162 the previous LHCb result and deviates from the SM prediction of lepton universality at the level of  
 163  $2.5\sigma$ .

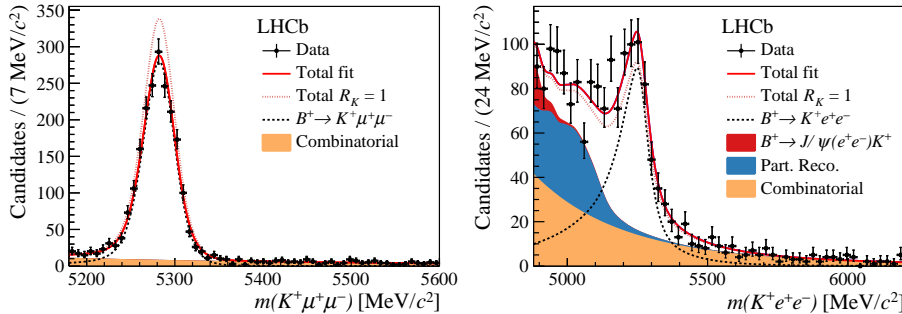


**Figure 5:** Invariant mass of  $K^+ \mu^+ \mu^-$  (left) and  $K^+ e^+ e^-$  (right) data candidates (black points) with the result of the invariant mass fit overlaid.

164 Belle has also recently published measurements of Lepton Universality with the ratios  $R_K$  and  
 165  $R_{K^*} = \mathcal{B}(B \rightarrow K^* \mu^+ \mu^-) / \mathcal{B}(K^* \rightarrow K^+ e^+ e^-)$  [27], using both the charged and neutral modes and  
 166 the full dataset. For  $R_{K^*}$  the  $K^*$  meson is reconstructed in the final states  $K^+ \pi^-$ ,  $K_S^0 \pi^-$  and  $K^+ \pi^0$ .  
 167 The ratios involving neutral hadrons in the final state are measured for the first time in this anal-  
 168 ysis. As a cross-check, the branching fraction of the control mode  $B \rightarrow K^* J/\psi$  is measured to  
 169 be in agreement with the world average and the ratio  $r_{J/\psi}$  is found to be in good agreement with  
 170 unity,  $r_{J/\psi} = 1.015 \pm 0.025 \pm 0.038$ , validating the efficiency determination. The signal yields are  
 171 extracted from a fit to the beam-constrained invariant mass of  $K^* \mu^+ \mu^-$  and  $K^* e^+ e^-$  candidates.  
 172 The main backgrounds are combinatorial, from particle misidentification and from decays involv-  
 173 ing charmonium resonances. Around 140  $B \rightarrow K^* \mu^+ \mu^-$  and 100  $B \rightarrow K^* e^+ e^-$  events are observed  
 174 in total. The ratio of branching fractions  $R_{K^*}$  is measured separately in the charged and neutral  
 175 modes in various  $q^2$  bins. All the values are found to be compatible with unity within uncertainties.  
 176 The results are also compatible with the existing and more precise LHCb measurement [6]. The  
 177 weighted average of the charged and neutral modes in the different  $q^2$  regions is shown in Fig. 6,  
 178 together with the previous results from LHCb and BaBar and the SM predictions.

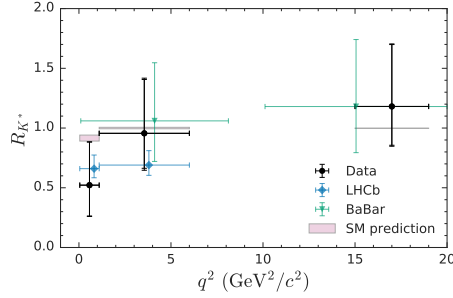


**Figure 6:** Charge-averaged  $R_{K^*}$  in bins of  $q^2$  as measured by Belle.

179 The Belle  $R_K$  measurement exploits a 3-dimensional fit of the beam-constrained mass, the  
 180 energy difference between the  $B$  candidate and the beam and the output of the multivariate classifier  
 181 used to separate signal and background. The measurement is also performed separately for the  
 182 charged and neutral modes and in different  $q^2$  regions. The charge average results are shown in  
 183 Fig. 7 (left) and are found to be compatible with the SM and also with the LHCb measurement  
 184 previously discussed. In the same analysis, Belle also measures the isospin asymmetry in

$$A_I = \frac{(\tau_{B^+} / \tau_{B^0}) \mathcal{B}(B^0 \rightarrow K^0 \ell \ell) - \mathcal{B}(B^+ \rightarrow K^+ \ell \ell)}{(\tau_{B^+} / \tau_{B^0}) \mathcal{B}(B^0 \rightarrow K^0 \ell \ell) + \mathcal{B}(B^+ \rightarrow K^+ \ell \ell)}, \quad (3.6)$$

185 where  $(\tau_{B^+} / \tau_{B^0}) = 1.076$  is the lifetime ratio of  $B^+$  to  $B^0$ . This observable is also measured in bins  
 186 of  $q^2$ . The results are found to be negative for almost all the  $q^2$  bins in both electron and muon  
 187 channels. The combined results are shown in Fig. 7 (right).

#### 188 4. Lepton Flavour Violation searches

189 Following the anomalies observed in  $b \rightarrow s \ell^+ \ell^-$  transitions, several new physics (NP) models  
 190 have been proposed to explain them. Specific examples can be found in Ref. [28]. Generally,



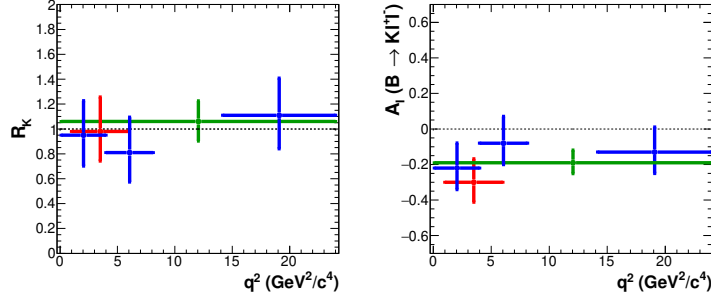


**Figure 7:** Charge-averaged  $R_K$  (left) and flavour-averaged  $A_I$  (right) in bins of  $q^2$  as measured by Belle.

191 models predicting lepton non-universality also imply lepton flavour violation, making the latter a  
 192 sensitive probe to these NP scenarios.

193 The decay  $B_{(s)} \rightarrow \tau \mu$  is forbidden in the SM but its branching fraction can be as large as  $10^{-4}$  in  
 194 NP models. For the  $B^0$  mode a limit was set by BaBar at  $\mathcal{B}(B^0 \rightarrow \tau \mu) < 2.2 \times 10^{-5}$  at 90% CL [29],  
 195 while no measurement is available for the  $B_s^0$  mode. Using the full Run 1 data, corresponding  
 196 to an integrated luminosity of  $3 \text{ fb}^{-1}$ , LHCb has performed a search for this decay exploiting the  
 197 hadronic tau decay  $\tau^- \rightarrow \pi^- \pi^+ \pi^- \nu_\tau$  and kinematic constraints on the event [30]. No signal excess  
 198 is observed in the region of interest so limits are set using the decay  $B^0 \rightarrow D^- (\rightarrow K^+ \pi^- \pi^-) \pi^+$  as  
 199 normalisation:

$$\begin{aligned} \mathcal{B}(B^0 \rightarrow \tau \mu) &< 1.2 \times 10^{-5} \\ \mathcal{B}(B_s^0 \rightarrow \tau \mu) &< 3.4 \times 10^{-5} \end{aligned} \quad (4.1)$$

200 at 90% CL, which are the most stringent limits to date.

201 The decay  $B^+ \rightarrow K^+ \mu e$  is also forbidden in the SM and can reach the level of  $10^{-8}$  in NP  
 202 scenarios. Previous constraints on this decay from BaBar set limits on the branching fraction at  
 203  $\mathcal{B}(B^+ \rightarrow K^+ \mu^- e^+) < 9.1 \times 10^{-8}$  and  $\mathcal{B}(B^+ \rightarrow K^+ \mu^+ e^-) < 13 \times 10^{-8}$  at 90% CL [31]. LHCb  
 204 has very recently performed a search for this decay using the Run 1 data [32]. The Bremsstrahlung  
 205 recovery procedure described above is used to correct the electron momentum and a two-stage  
 206 multivariate selection is employed to reduce the background from combinatorial and partially re-  
 207 constructed  $b$ -hadron decays. No signal excess is observed and limits on the branching fraction are  
 208 derived using the  $B^0 \rightarrow J/\psi K^+$  decay as normalisation:

$$\begin{aligned} \mathcal{B}(B^+ \rightarrow K^+ \mu^- e^+) &< 7.0 \times 10^{-9} \\ \mathcal{B}(B^+ \rightarrow K^+ \mu^+ e^-) &< 7.1 \times 10^{-9} \end{aligned} \quad (4.2)$$

209 at 90% CL, which are the most stringent limits to date, improving by more than an order of magni-  
 210 tude the previous constraints.

## 211 5. Summary

212 Rare decays of  $b$ -hadrons provide high sensitivity to NP effects. Several deviations with respect  
 213 to the SM predictions have been observed in recent years, leading to significant tensions in

214 global fit analyses. The latest results from LHCb and Belle on radiative, penguin semileptonic and  
 215 lepton flavour violation decays are presented. These involve improvements on the constraints on  
 216  $C_7'$ , complementary angular distribution measurements and further tests of lepton flavour univer-  
 217 sality in  $b \rightarrow s \ell^+ \ell^-$  transitions and new or largely improved constraints on lepton flavour violating  
 218 decays. The tensions in  $b \rightarrow s \ell^+ \ell^-$  processes with respect to the SM predictions remain after these  
 219 results, motivating further updates with larger datasets and the exploration of new modes. LHCb  
 220 has already collected data corresponding to  $9 \text{ fb}^{-1}$ , a good part of which remains to be analysed,  
 221 and both Belle II and LHCb will collect much larger datasets in the coming years, which will allow  
 222 to clearly disentangle the presence and nature of new physics if the current observed anomalies are  
 223 indeed originated by physics beyond the SM [33, 34].

## 224 References

- 225 [1] R. Aaij et al. (LHCb Collaboration), Differential branching fractions and isospin asymmetries of  
 226  $B \rightarrow K^* \mu^+ \mu^-$  decays, *JHEP06(2014)133*, [arXiv:1403.8044](#).
- 227 [2] R. Aaij et al. (LHCb Collaboration), Angular analysis and differential branching fraction of the decay  
 228  $B_s^0 \rightarrow \phi \mu^+ \mu^-$ , *JHEP09(2015)179*, [arXiv:1506.08777](#).
- 229 [3] R. Aaij et al. (LHCb Collaboration), Differential branching fraction and angular analysis of  
 230  $\Lambda_b^0 \rightarrow \Lambda \mu^+ \mu^-$  decays, *JHEP06(2015)115*, [arXiv:1503.07138](#), Erratum *JHEP09(2018)145*.
- 231 [4] R. Aaij et al. (LHCb Collaboration), Angular analysis of the  $B^0 \rightarrow K^{*0} \mu^+ \mu^-$  decay using  $3 \text{ fb}^{-1}$  of  
 232 integrated luminosity, *JHEP02(2016)104*, [arXiv:1512.04442](#).
- 233 [5] R. Aaij et al. (LHCb Collaboration), Test of lepton universality using  $B^+ \rightarrow K^+ \ell^+ \ell^-$  decays,  
 234 *JHEP09(2015)179*, [arXiv:1406.6482](#).
- 235 [6] R. Aaij et al. (LHCb Collaboration), Test of lepton universality with  $B^0 \rightarrow K^{*0} \ell^+ \ell^-$  decays,  
 236 *JHEP08(2017)055*, [arXiv:1705.05802](#).
- 237 [7] R. Aaij et al. (LHCb Collaboration), First experimental study of photon polarization in radiative  $B_s^0$   
 238 decays, *Phys. Rev. Lett.* **118**.021801.
- 239 [8] R. Aaij et al. (LHCb Collaboration), Measurement of CP-violating and mixing-induced observables in  
 240  $B_s^0 \rightarrow \phi \gamma$  decays, *Phys. Rev. Lett.* **123**.081802.
- 241 [9] Y. Wang, Y. Li and C. Lü, Rare decays of  $\Lambda_b^0 \rightarrow \Lambda \gamma$  and  $\Lambda_b^0 \rightarrow \Lambda \ell \ell$  in the light-cone sum rules, *Eur.*  
 242 *Phys. J. C* **59**:861-882, 2009, [arXiv:0804.0648](#).
- 243 [10] T. Mannel and Y. Wang, Heavy-to-light baryonic form factors at large recoil, *JHEP12(2011)067*,  
 244 [arXiv:1111.1849](#).
- 245 [11] L. Gan, Y. Liu, W. Chen and M. Huang, Improved light-cone QCD sum rule analysis of the rare  
 246 decays  $\Lambda_b^0 \rightarrow \Lambda \gamma$  and  $\Lambda_b^0 \rightarrow \Lambda l^+ l^-$ , *Commun. Theor. Phys.*, **58**:872-882, 2012, [arXiv:1212.4671](#).
- 247 [12] R. N. Faustov and V. O. Galkin, Rare  $\Lambda_b^0 \rightarrow \Lambda l^+ l^-$  and  $\Lambda_b^0 \rightarrow \Lambda \gamma$  decays in the relativistic quark  
 248 model, *Phys. Rev. D* **96**.053006, [arXiv:1705.07741](#).
- 249 [13] D. Acosta et al. (CDF Collaboration), Search for radiative b-hadron decays in  $p\bar{p}$  collisions at  $\sqrt{s} =$   
 250  $1.8 \text{ TeV}$ , *Phys. Rev. D* **66**.112002, [arXiv:hep-ex/0208035](#).
- 251 [14] T. Mannel and S. Recksiegel, Flavour-changing neutral current decays of heavy baryons. The case  
 252  $\Lambda_b^0 \rightarrow \Lambda \gamma$ , *J. Phys.*, **G24**:979-990, 1998., [arXiv:hep-ph/9701399](#).

- 253 [15] R. Aaij et al. (LHCb Collaboration), First observation of the rare radiative  $\Lambda_b^0 \rightarrow \Lambda \gamma$  decay.
- 254 [16] T. Chen and C. Guestrin, XGBoost: A Scalable Tree Boosting System, [Proceedings of the 22Nd ACM](#)  
255 [SIGKDD International Conference on Knowledge Discovery and Data Mining](#).
- 256 [17] M. Calvo Gomez et al., A tool for  $\gamma/\pi^0$  separation at high energies, [LHCb-PUB-2015-016](#).
- 257 [18] R. Aaij et al. (LHCb Collaboration), Measurement of  $b$ -hadron fractions in 13 TeV  $pp$  collisions,  
258 [arXiv:1902.06794](#).
- 259 [19] M. Tanabashi et al. (Particle Data Group), [Review of particle physics](#), *Phys. Rev. D* **98**.030001.
- 260 [20] R. Aaij et al. (LHCb Collaboration), Angular moments of the decay  $\Lambda_b^0 \rightarrow \Lambda \mu^+ \mu^-$ ,  
261 [JHEP09\(2018\)146](#), [arXiv:1808.00264](#).
- 262 [21] T. Blake and M. Krepes, Angular distribution of polarised  $\Lambda_b$  baryons decaying to  $\Lambda \ell^+ \ell^-$ ,  
263 [JHEP11\(2017\)138](#), [arXiv:1710.00746](#).
- 264 [22] D. van Dyk, C. Bobeth, F. Beaujean and T. Blake, EOS – A HEP program for flavor observables,  
265 <https://doi.org/10.5281/zenodo.886055>, <https://eos.github.io>.
- 266 [23] R. Aaij et al. (LHCb Collaboration), Measurements of the  $\Lambda_b^0 \rightarrow J/\psi \Lambda$  decay amplitudes and the  $\Lambda_b^0$   
267 polarisation in  $pp$  collisions at  $\sqrt{s} = 7$  TeV, *Phys. Lett. B* **05**:041, 2013, [arXiv:1302.5578](#).
- 268 [24] M. Bordone, G. Isidori and A. Pattori, On the Standard Model predictions for  $R_K$  and  $R_{K^*}$ , *Eur.Phys.J.*  
269 *C* **76** (2016) no.8, 440.
- 270 [25] R. Aaij et al. (LHCb Collaboration), Search for lepton-universality violation in  $B^+ \rightarrow K^+ \ell^+ \ell^-$   
271 decays, *Phys. Rev. Lett.* **122** (2019) 191801.
- 272 [26] A. Abdesselam et al. (Belle Collaboration), Test of lepton flavor universality in  $B \rightarrow K \ell^+ \ell^-$  decays,  
273 [arXiv:1904.02440](#).
- 274 [27] A. Abdesselam et al. (Belle Collaboration), Test of lepton flavor universality in  $B \rightarrow K^* \ell^+ \ell^-$  decays  
275 at Belle, [arXiv:1904.02440](#).
- 276 [28] M. Blanke, Constraints on New Physics from B decays, [This proceedings](#).
- 277 [29] B. Aubert et al. (BaBar Collaboration), Searches for the decays  $B^0 \rightarrow \ell^\pm \tau^\mp$  and  $B^+ \rightarrow \ell^+ \nu$  ( $\ell = e, \mu$ )  
278 using hadronic tag reconstruction, *Phys.Rev.D* **77** 091104 2008.
- 279 [30] R. Aaij et al. (LHCb Collaboration), Search for the lepton-flavour-violating decays  $B_s^0 \rightarrow \tau^\pm \mu^\mp$  and  
280  $B^0 \rightarrow \tau^\pm \mu^\mp$ , [arXiv:1905.06614](#).
- 281 [31] B. Aubert et al. (BaBar Collaboration), Measurements of branching fractions, rate asymmetries, and  
282 angular distributions in the rare decays  $B \rightarrow K \ell^+ \ell^-$  and  $B \rightarrow K^* \ell^+ \ell^-$ , *Phys.Rev.D* **73** 092001 2006.
- 283 [32] R. Aaij et al. (LHCb Collaboration), Search for the lepton-flavour violating decays  $B^+ \rightarrow K^+ \mu^\pm e^\mp$ ,  
284 [arXiv:1909.01010](#).
- 285 [33] W. Altmannshofer et al. (Belle II Collaboration), The Belle II Physics Book, [arXiv:1808.10567](#).
- 286 [34] R. Aaij et al. (LHCb Collaboration), Physics case for an LHCb Upgrade II - Opportunities in flavour  
287 physics, and beyond, in the HL-LHC era, [arXiv:1808.08865](#).